

ON REMOTE DETECTION OF SPATIAL ANOMALIES OF THE WAVY SEA SURFACE

B.D. Borisov and V.A. Krutikov

*Institute of Atmospheric Optics,
Siberian Branch of the Russian Academy of Sciences, Tomsk
Received December 6, 1994*

Preliminary night-time experimental results of airborne remote diagnostics of the wavy sea surface state are discussed in the paper. The results were obtained by frame-by-frame statistical processing of TV images recorded with illumination of the sea surface by a directional optical pulse. The estimates of spatial amplitude and frequency characteristics and autocorrelation function of the image structure are treated and their informative parameters are compared for background wind-driven sea waves and in the wake of sailing ship.

Considerable attention has been given to the development of methods and means for remote sounding of the sea surface to study the spatiotemporal parameters of roughness over a sufficiently large area for various practical applications.¹⁻⁵ In many cases there is a need for real-time recording and analysis of characteristics of spatial distribution of small-scale roughness and in particular for detection of areas anomalous in structure of the wavy sea surface (SS) against the background of free wind-driven waves. These phenomena occur, for example, due to interaction between internal waves and surface waves when the transformation of spectrum of short surface waves is of primary importance. The regime of surface roughness also changes under the effect of oil films and surface acoustic wave (SAW).

The real-time information about the state of the atmosphere-ocean interface is also necessary to solve such scientific and applied problems as the study of surface wave dynamics, currents, and circulations on the sea surface, the detection of wakes of sailing ships, etc. Moreover, practical implementation of the methods of remote sensing calls for the night-time observations as well as those through mist and smoke.

In daylight the methods of analyzing the spatial spectra of SS optical image⁵ are successfully used to solve the aforementioned problems. For a large number of bright spots in sunlight the transfer function that converts the fields of elevations and slopes of the sea surface into the fields of image brightness is substantially nonlinear and therefore one must develop special methods for solving this problem.⁶ The similar situation arises when this problem is solved for night-time observations with pulsed optical illumination.⁷

As is seen, the remote sensing of SS is very actual and covers a wide class of problems. If we restrict ourselves to the problem of searching a method for real-time detection of the region of anomalous surface waves using hardware, the statement of the problem will be simplified. Let us now consider the possible night-time detection of smooth surface or bright spot on SS in the example of the turbulent wake of a ship in the open ocean.

The brightness field structure of the sea surface with its pulsed illumination by a source having small angular dimensions (dimensions of emitter are much smaller than the distance to the examine plane) at night differs substantially from that in natural daylight (i.e., illumination by an extended source). This is primarily due to different conditions of illumination since with directional

illumination the main contribution to the recorded image comes from bright spots appearing at the points of the sea surface (facets) at which the condition of specular reflection is fulfilled. For real observational systems the recorded brightness field, in addition to the SS state, is determined by the source directional pattern and the receiver field of view (angles of incidence and reflection of illumination with the surface under study). With nadir pulsed illumination, the signal bright spot component in the image plane is formed within a solid angle whose vertex is at the SS point from which the illumination source is seen.

Between the Cartesian coordinates of the points on SS and the slopes of the surface elements (deflection of the normal to element area from the vertical axis) that produce bright spots at this point there is a one-to-one correspondence determined by the geometric parameters of an observational system. In this case there are no requirements for angular uniformity of the directional pattern and no limitations on the pulse shape of illumination source since the spatial position of a spot is recorded against the scattered radiation background. This peculiarity of images recorded with illumination of SS by a pulsed source having small angular dimensions allows one to use them to estimate the distribution density of wavy SS slopes.

Direct experimental measurements reported in Ref. 8 showed that in the region of free wind-driven waves (region of background roughness) the distribution functions of sea surface slopes is approximated by a two-dimensional normal distribution (with a certain correction to a square power term). However, the data on length, lifetime, and behavior of turbulent wakes of ships under different weather conditions,³ not to mention their images recorded from onboard the airplanes, are unavailable in the literature. Therefore, it was necessary to carry out preliminary field observations of the wavy SS structure to assess the feasibility of detection of its spatial night-time anomalies as well as to determine the acceptable characteristics and distinguishing features that could allow one to detect automatically such anomalies. To this end, the flight mission was undertaken over the open sea. To record a particular series of SS images both in the region of background roughness and outside it, we either followed the ship course or traverse the ship wake. Eight 10 km tacks, which provided a series of spatial images, were made. The flight height was 300 m with a mean aircraft velocity of 300 km/hr. With pulsed optical illumination of the sea surface, the brightness field of SS images was recorded by

an aircraft TV system in standard or synchronous frame-wise (recording of individual frames) regimes with analog storage of signal on a videorecorder and temporal fixation of the signal to a reference point on a flight trajectory and thus to spatial position with respect to a sailing ship. Subsequent digitizing and statistical frame-by-frame processing of information were made on a ground-based computer system.

Figure 1 shows a block diagram of instrumental complex placed onboard the AN-30 aircraft. A signal from synchronizing contacts of a frame-wise TV camera or a signal of automated triggering in standard TV recording regime is fed into the control unit 2 connected with the power supply unit 1 of illuminating system and starts a radiation source (IFK-150 pulsed xenon-filled lamp). A parabolic reflector of diameter 450 mm provides a 15° angular width of the directional pattern of the illumination source. The illumination pulse duration was 300 μs, the pulse repetition frequency did not exceed 2 Hz. A frame identification pulse from the control unit 2 is synchronously fed into the videorecorder.³ The vidicon TV camera 5 with the power supply unit 4 operates in the preset recording mode. A signal is continuously stored on an analog videorecorder. A video image is controlled with the video control unit 6. The instrumental complex operates off the onboard mains through the distributor 7. The field of view of the receiving TV system with a standard objective is 10°×13°. It provides a record of a 100×140 m surface area in a single frame at 300 m flight height and is nearly optimal for receiving the bright-spot component of a signal from the wavy sea surface by physical reasoning of image formation described above.

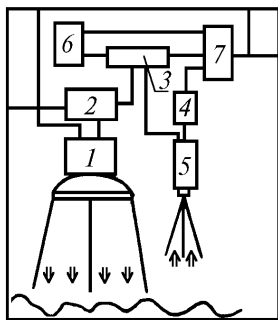


FIG. 1. Block diagram of the aircraft instrumental complex.

A system of image graphics, graphics digitizer, and preliminary processing of image was used to process the analog TV information obtained in flight. Storage of an image frame could be controlled by an automated program or by a synchronizing pulse of the recorded frame identification. The TV images of the sea surface were directly processed by a videoprocessor with a computer-controlled multipurpose analog-to-digital converter⁹ (ADC). A 8-bit ADC accomplishes the TV signal quantization into 256 levels. The spatial size of the image processing window was 512×512 pixels, what determines not only the scale of the investigated spatial characteristics of the wavy SS structure, but also all linear dimensions on the surface under study with allowance for changes in course, height, and velocity of flight during measurements. In processing, most important was the signal produced by illumination pulse after reflection from facets recorded against the background level created by pulsed radiation scattering in the water and the atmosphere. Therefore, during the processing we used cross-sectional mapping of brightness contours at different levels of quantization of the recorded image. We selected 236 reference

frames of TV images displaying a series of recorded pulsed optical images for eight tacks of aircraft flight to make preliminary choice of informative parameters that can be used to detect the wake of a ship from the images of SS brightness fields.

The software of a specified videoprocessing system was based on algorithms for computing the probabilistic characteristics of discrete images of random fields.¹⁰ Programs for processing the TV images of the pulsed SS brightness field were used to compute the central moments of arbitrary order and spatial spectra of brightness field distribution for different (of the 256 possible) cross-sectional maps of brightness contours. In the preliminary qualitative comparative analysis, we used spatial autocorrelation function and frequency characteristics (two-dimensional Fourier spectrum) of digitized SS images as well as the simplest characteristic of bright-spot distribution in the plane, namely, the dispersion ellipse. The computed functions were displayed in pseudocolors on the screen of a color monitor in order of processing of digital arrays for each frame for a given level of brightness contour of cross-sectional map.

An analysis of the available experimental material has shown that as the wavy SS structure changes, a visual set of bright spot surface elements that can be approximated with the ellipse also changes. On the assumption of the normal law of bright-spot distribution in the Cartesian system of coordinates in the image plane, the following parameters of the dispersion ellipse were estimated: the standard deviations σ_ξ and σ_η (axial lengths of ellipse in the directions ξ and η), the angle α determining the orientation of the major axis of the ellipse, and the coordinates of its center m_x and m_y in the observation plane.¹¹ For convenience of comparison in data processing, the coordinate axes in the image plane were chosen so that the ordinate (the y -axis) was aligned with the aircraft flight course, and the spatial orientation of the ellipse was then corrected with allowance for the course angle of the aircraft.

By way of example, Table I lists the parameters of dispersion ellipses for a signal discretization level of 210 and different flight courses: tack No. 1 (course of 270°, flight counter to the ship), tack No. 2 (course of 300° that traverses the wake at a 500 m distance from the ship), and tack No. 7 (course of 90°, flight follows the course the ship). Displayed for each tack is the result of processing of three image frames, each second recorded in the region of anomalous structure (turbulent wake) of the surface roughness. The orientation of the major axes of dispersion ellipses of the optical image of the totality of bright spots on SS was converted to the aircraft course angle.

TABLE I.

Course deg.	Tack	Serial number of file	Orientation of the major axis of dispersion ellipse (course angles)	Parameters of dispersion ellipse (arbitrary units)	
				σ_ξ	σ_η
270	1	97	315	$3.7 \cdot 10^4$	$2.1 \cdot 10^4$
		99	139	$3.9 \cdot 10^3$	$9.4 \cdot 10^2$
		102	197	$5.6 \cdot 10^4$	$4.9 \cdot 10^4$
300	2	200	327	$4.6 \cdot 10^4$	$6.9 \cdot 10^4$
		202	170	$2.8 \cdot 10^2$	$4.4 \cdot 10^3$
		204	326	$1.3 \cdot 10^5$	$6.8 \cdot 10^4$
90	7	901	31	$5.1 \cdot 10^4$	$3.0 \cdot 10^4$
		904	205	$1.2 \cdot 10^2$	$3.8 \cdot 10^3$
		906	12	$2.3 \cdot 10^5$	$2.1 \cdot 10^5$

As seen from the table, the axial lengths (standard deviations) of the dispersion ellipses in the region of background roughness differ slightly and correspond to an isotropic character of roughness. In the region of turbulent wake the major axis lengths decrease nearly by an order of magnitude, elongation of the dispersion ellipse becomes stronger, and orientation of the major axis changes. Such variation of the parameters of recorded bright spot distribution over the area is caused by high damping of the water surface waves immediately behind a sailing ship, i. e., a locally smooth surface is formed. In this case most of specularly reflecting surface elements orient their normals nearly along the receiver optical axis, the source image is formed by slightly diverging beams, and its visible size decreases.

Thus, when the smooth surface element appears on the sea surface, the parameters of dispersion ellipse for bright spot components decrease, and in case of a sufficiently smooth specularly reflecting surface it degenerates into a circle whose radius is close to angular dimensions of the radiation source. Such results were observed in our experiments over lakes whose surface was in practically unperturbed state. Therefore, in general such a characteristic of the wavy SS structure as a dispersion ellipse is insufficient for confident and reliable detection of anomalies in the background structure of SS with its pulsed illumination. This characteristic can be used in the turbulent wake of a sailing ship not very far from the ship, with sharply pronounced anisotropy in the surface wave structure.

Computation and analysis of the spatial Fourier spectra obtained using standard algorithms of a two-dimensional fast Fourier transform (TDFFT) that are popular in daytime remote measurements of the parameters of roughness by the method of aerophotography² also turned out to be inefficient for the solution of this problem. This is accounted for by a specific pattern of image of the pulsed field of SS brightness, with the spatial distribution of the signal reflected from bright spots playing the dominant role. Discontinuities in the SS image brightness function result in occurrence of large components at high spatial frequencies of the spectrum. Moreover, with substantial smoothing of the surface in the region of anomalies, where the number of bright spots and their total area decrease, the spatial frequency characteristic (SFC) retains similarity and has no distinct informative characteristics. An analysis of the obtained experimental material showed that really the SFC of brightness fields of strongly different surfaces substantially overlap, and the SFC without special processing has no additional informative parameters as compared with the dispersion ellipse. For example, if the scale of the spatial spectrum (i.e., its width in the window under processing 512×512 pixels), which changes for some regions of the turbulent wake is assumed to be an informative parameter, then such information about the wake also can be obtained from the parameters of the dispersion ellipse. Taking into account that the execution time and resources in the first and second cases are incomparable, we see little reason in the use of SFC for extracting the information about the SS structure with its pulsed illumination.

Another characteristic chosen for an analysis of the image of the SS pulsed brightness field is the spatial

autocorrelation function. It is computed at each point (ξ, η) of a $(2N + 1) \times (2N + 1)$ digital array of image pixels with successive shift $k, l = 0, \pm 1, \pm 2, \dots, \pm N$:

$$R(k, l; \xi, \eta) = \frac{\sum_{m=\xi-N}^{\xi+N} \sum_{n=\eta-N}^{\eta+N} g(m, n) g(m-k, n-l)}{\sum_{m=\xi-N}^{\xi+N} \sum_{n=\eta-N}^{\eta+N} [g(m, n)]^2}.$$

As follows from general properties of correlation functions, for fixed shift (k, l) a larger value of the spatial autocorrelation function (SACF) is obtained for a region of large-scale roughness. Thus, the scale of roughness is proportional to the SACF width, and the surface structure can be described by the absolute statistical moments of the correlation functions.

An analysis of the experimental data showed that the SACF of the SS brightness field image has the highest sensitivity to variations in the roughness structure. In going from the region of background roughness to the region of anomalies and wakes, the SACF image often clustered. As the distance from the perturbation source increases, the high-frequency component of roughness appears again under the effect of wind structure, and large-scale smoothing takes place.

By way of example, Figs. 2 and 3 display a fragment of successive processing of the videofilm (digital image of SS, spatial Fourier spectrum, and autocorrelation function of the SS image) made in the experiment with the aircraft flight counter the ship. The first three frames of a series (Fig. 2) display the SS brightness field image and its spatial characteristics in front of the ship bow, the second three frames (Fig. 3) display those behind the ship stern. Next frames (Fig. 4) display only SACF of the SS image for the same realization as that in Figs. 2 and 3 in the wake as the distance from the ship increases (for SACF, a fragment of a series is displayed in Figs. 2c and 3c and then in Fig. 4 from top to bottom). It should be noted that each of the examined image frames is a fragment of spatial SS image with corresponding position with respect to the sailing ship.

The examples of correlation functions of the wavy SS structure in different perturbation regions for the remaining three tacks are displayed in Figs. 5–7, respectively.

The frames for one tack are arranged in the following order: the upper image of pair of fragments of the videofilm processing displays unperturbed (background) wavy SS, the lower image displays the region of anomalous perturbation in the turbulent wake behind the ship stern. Figure 5 displays SACF's for tack No. 1, course of 270°, i.e., flight opposite the ship. Figures 6 and 7 display analogous data for tack No. 2, course of 300°, aircraft traverses the wake at a distance of about 500 m from the ship stern, and tack No. 7, course of 90°, aircraft follows the ship course. These data clearly illustrate the reaction of SACF of the SS pulsed brightness field image to variations in the roughness structure.

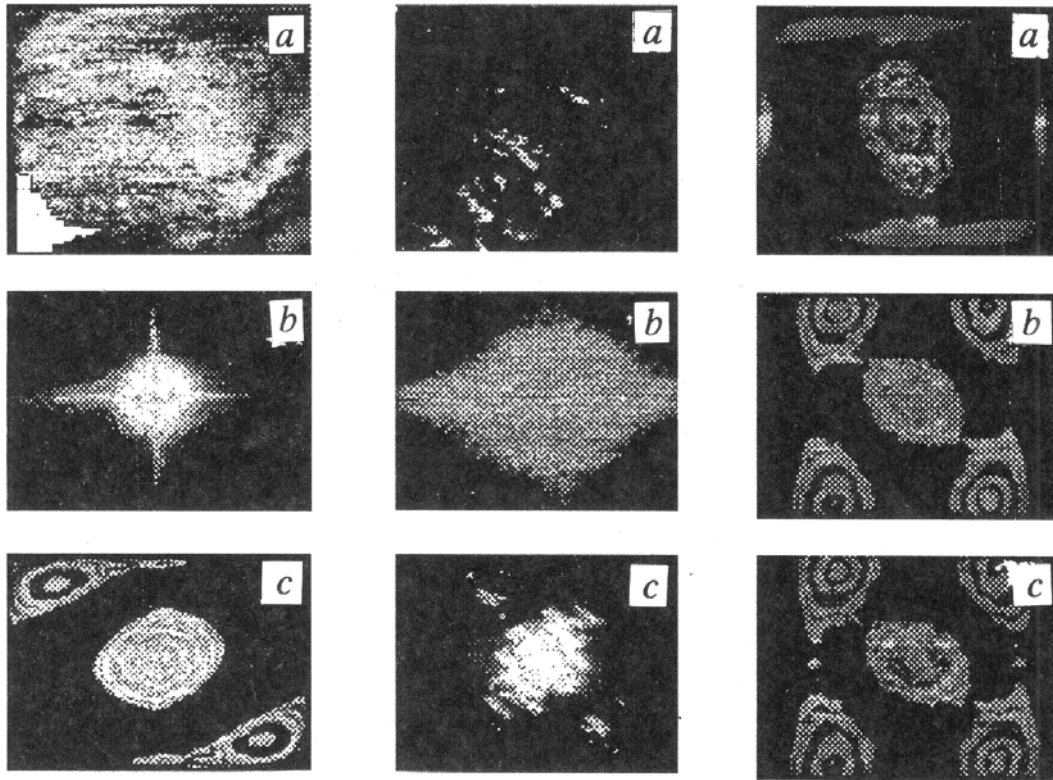


FIG. 2.

FIG. 2. Images of the sea surface (SS), spatial frequency characteristic (SFC), and spatial autocorrelation function (SACF) in the region of background roughness.

FIG. 3.

FIG. 3. Images of SS, SFC, and SACF in the region of the wake.

FIG. 3.

FIG. 4. Image of SACF in the region of wake as the distance from the ship stern increases.

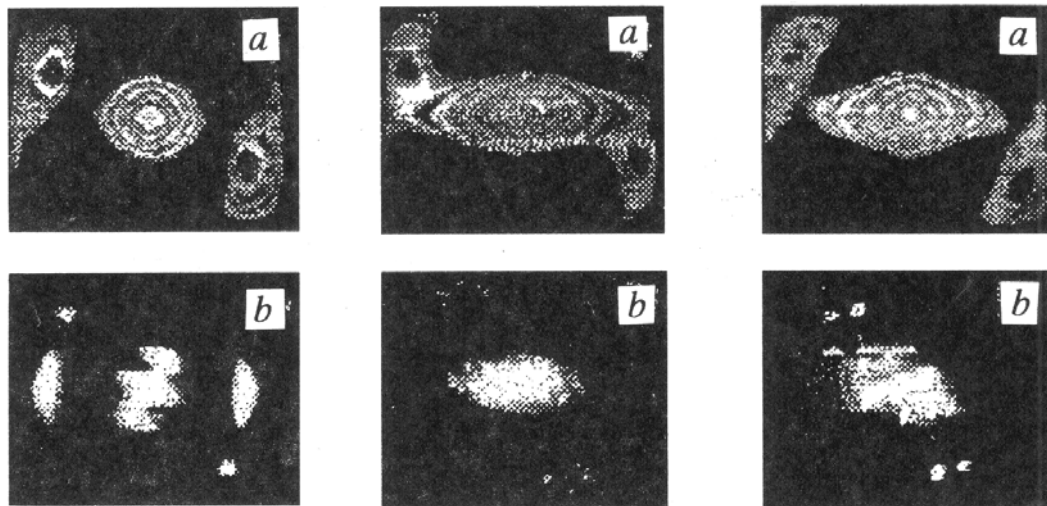


FIG. 5.

Fig. 5. Images of SACF in the background region and in the wake (flight counter the ship).

FIG. 6.

Fig. 6. Image of SACF in the background region and in the wake (the aircraft traverses the course at a 500 m distance from the ship stern).

FIG. 7.

Fig. 7. Image of SACF in the background region and in the wake (flight follows the ship course).

Thus, the spatial autocorrelation function retrieved from the images of the discrete brightness field of the wavy sea surface with its pulsed illumination can be used to identify the SS structure in real time. In so doing the main distinctive feature is the shape and internal structure of the SACF visual image in the background region of free wind-driven waves and under conditions of smoothing, turbulent wake, smooth surface, and other anomalies on SS. The SACF patterns considered in the analysis of the experimental data suggest that the central part of a plane singular figure displaying calculated results can be used as the fundamental and most specific parameter of SACF of background roughness. For SACF of background roughness in most cases a family of contours of the image with equal levels of brightness displayed for shifts $0 \leq (k, l) \leq 170$ of digital counts can be approximated by second-order curves. Configurations of brightness contours for shifts $(k, l) > 170$ acquire different shapes. In this case the correlation regions of opposite points of the images can be adjacent to or separated from the central fragment of the background roughness SACF figure. The patterns of background roughness SACF, in the overwhelming majority of cases display no more than two symmetrically located fragments for large shifts (k, l) . The analysis carried out during this experiment allow us to give the simplest classification of correlation functions. Figures 2c, 5a, 6a, and 7a display typical results of SACF calculation for background images of SS with its pulsed illumination.

Since the basic informative characteristics of the wavy sea surface structure derived by processing of its optical image recorded with its pulsed vertical illumination are related to spatial position of bright spots rather than to the energy of reflected radiation, it is expedient to convert the initial image (minus the scattered radiation background) into binary spatial distribution being equal to 0 without a bright spot on the image pixel and 1 when it appears. This procedure can be easily realized during image graphics and digitizing, it makes further processing easier and enables us to compute the spatial autocorrelation function using high-speed microprocessors. Numerical processing of the recorded video images demonstrated the efficiency of the aforementioned algorithm and its possible application to optical signal processing in real time. A binary optical

signal is easily filtered from the distorting effect of the scattering atmosphere since the outer image scale (low-frequency component of optical signal) is distorted by the atmosphere to the least extent.

It can be concluded that usage of the spatial autocorrelation function of optical image as an informative parameter for detecting anomalies in the background structure of the wavy sea surface with its pulsed illumination is promising. It should be noted that the classification of SACF for different regions of roughness required to develop systems of automated detection of anomalies on the wavy SS must be discussed specially based on the results of detailed field experiments.

REFERENCES

1. A.S. Monin, ed., *Oceanic Optics* (Nauka, Moscow, 1983), Vol. 2, 236 pp.
2. A.A. Zagorodnikov, *Airborne Radar Measurements of Sea Surface Roughness* (Gidrometeoizdat, Leningrad, 1978), 239 pp.
3. A.C. Monin and V.P. Krasitskii, *Phenomena on Oceanic Surface* (Gidrometeoizdat, Leningrad, 1985), 375 pp.
4. F.V. Bunkin, K.I. Volyak, A.I. Malyarovskii, et al., *Dokl. Akad. Nauk SSSR* **281**, No. 6, 1441–1445 (1985).
5. V.G. Bondur, in: *Opto-Meteorological Studies of the Earth's Atmosphere* (Nauka, Novosibirsk, 1987), pp. 217–230.
6. A.B. Murynin and E.A. Lupyan, *Atm. Opt.* **3**, No. 3, 264–270 (1990).
7. V.G. Bondur, B.D. Borisov, V.N. Genin, et al., in: *Image Transfer in the Earth's Atmosphere* (Tomsk Affiliate of the Siberian Branch of the Academy of Sciences of the USSR, Tomsk, 1988), pp. 42–45.
8. C. Cox and W. Munk, *J. Opt. Soc. Am.* **44**, No. 11, 838–850 (1954).
9. V.I. Zhuravlev, S.L. Shinkevich, V.A. Gridnev, et al., in: *Problem-Oriented Measuring-Computational Systems* (Nauka, Novosibirsk, 1986), pp. 58–62.
10. W. Pratt, *Digital Image Processing* (Wiley, New York, 1978).
11. G. Korn and T. Korn, *Mathematical Handbook for Scientists and Engineers* (McGraw Hill, New York, 1961).